Research Article Vol. 57, No. 9 / 20 March 2018 / Applied Optics 2007

applied optics

Holographic waveguide heads-up display for longitudinal image magnification and pupil expansion

Colton M. Bigler,[1,*] Pierre-Alexandre Blanche,[1] and Kalluri Sarma[2]

[1]College of Optical Sciences, University of Arizona, 1630 E. University Blvd., Tucson, Arizona 85719, USA
[2]Honeywell, Advanced Technology, 21111 N. 19th Avenue, M/S 2J35, Phoenix, Arizona 85027, USA
*Corresponding author: cbigler@optics.arizona.edu

Received 6 November 2017; revised 7 February 2018; accepted 8 February 2018; posted 8 February 2018 (Doc. ID 312726); published 12 March 2018

The field of view of traditional heads-up display systems is limited by the size of the projection optics. Our research is focused on overcoming this limitation by coupling image-bearing light into a waveguide using holographic elements, propagating the light through that waveguide, and extracting the light several times with additional holographic optical elements. With this configuration, we demonstrated both longitudinal magnification and pupil expansion of the heads-up display. We created a ray-trace model of the optical system to optimize the component parameters and implemented the solution in a prototype that demonstrates the merit of our approach. Longitudinal magnification is achieved by encoding optical power into the hologram injecting the light into the waveguide, while pupil expansion is obtained by expanding the size of the hologram extracting the light from the waveguide element. To ensure uniform intensity of the image, the diffraction efficiency of the extracting hologram is modulated according to the position. Our design has a 12° × 8° field of view at a viewing distance of 10 in. (250 mm), with infinite longitudinal magnification and a 1.7× lateral pupil expansion.

OCIS codes: (090.2820) Heads-up displays; (090.2870) Holographic display.

https://doi.org/10.1364/AO.57.002007

1. INTRODUCTION

Heads-up displays (HUDs) provide major advantages, during operations requiring out-the-window viewing, over traditional head-down displays (HDD) displays, including shorter accommodation time, increased eyes-forward time, improved situational awareness, faster reaction time, and ease of use [1,2]. By overlaying relevant flight data on the real-world scene outside the plane, pilots are saved from having to redirect their gaze from the exterior of their vehicle to see the information on the HDDs [3–5]. HUDs designed for aviation locate their projected flight symbols in the far field [6,7]. This means that observers need not change their focus away from their environment to see the information presented by the HUD. HUD systems in aircraft or other vehicles frequently use a projection system similar to that shown in Fig. 1, where the source is imaged by a collection of projection optics onto the combiner and redirected from there to the pilot's eyes [8–13].

One of the primary limitations of the system shown in Fig. 1 is that the maximum extent of the projected image is determined by the projection optics encompassed in the "packaged volume" [14–16]. To increase the size of the perceived image, the size of these optical elements must be increased. Because most vehicles have a limitation on the space they can allocate to housing an HUD system, increasing the size of the projection optics quickly becomes an unreasonable proposition. Additionally, because of the projection mechanism used in this configuration, pilots have a very small eyebox from which they can observe the entire HUD image. The "eyebox" refers to the area where an observer can situate his/her head and see the entire projected image. When the observer moves his/her eyes outside the eyebox, the image starts to be clipped by the edge of the aperture. Ultimately, larger head movements cause the image to disappear completely.

To overcome these limitations, recent research has proposed the use of diffractive optics in combination with waveguides to increase the eyebox of HUD systems [17–21]. By using holograms to couple the light into a waveguide, the image is propagated within the waveguide and extracted multiple times, allowing for an increased eyebox. Figure 2 shows this configuration, where several holograms and waveguides are used in conjunction to achieve two-dimensional (both lateral and vertical) pupil expansion.

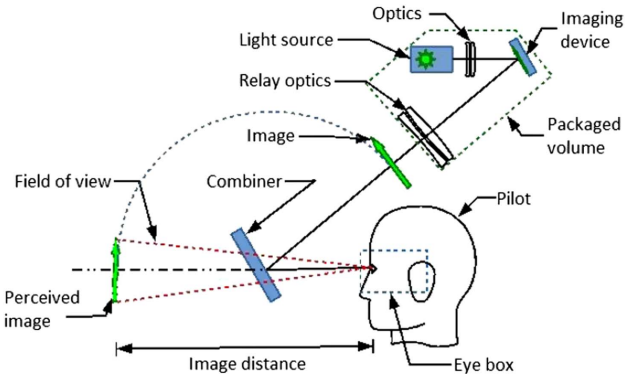

Fig. 1. Conventional HUD system schematic where the projected image is propagated to the combiner. From there, it is reflected into the user's eyes. The viewer sees the image located in the far field in front of him/her.

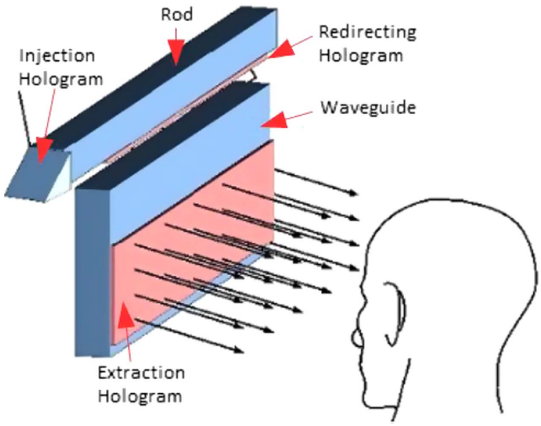

Fig. 2. Propagation through the waveguides allows for two-dimensional pupil expansion.

The holographic elements shown in Fig. 2 function as partially reflective elements. By modulating the diffraction efficiency (DE), it is possible to achieve uniform intensity of the light observed across an expanded pupil. In addition, holograms can also be recorded with optical power, which allows for image expansion. Both of these techniques are used in this article to achieve both longitudinal image magnification and pupil expansion in an HUD system.

2. SYSTEM DESIGN

This research worked to design a waveguide HUD for implementation in civilian aircraft; however, the principle can be used in a wide variety of applications, including automobiles. Our system is comprised of an injection and extraction hologram pair attached to a planar waveguide surface. The injection hologram accepts an incident beam of light and redirects it inside the waveguide beyond the critical angle. This causes the beam to reflect within the waveguide surface, due to total internal reflection (TIR). In this case, our waveguide and photopolymer have refractive indices of 1.526 and 1.485, respectively. This gives us a critical angle of 40.9°. After propagating within the waveguide, the beam reaches the extraction hologram, where it is redirected out of the waveguide and toward the observer. Figure 3 shows the beam path within the waveguide. A collimated beam incident on the hologram surface is redirected within the glass at TIR. This beam propagates until the extraction hologram redirects it out of the waveguide. The modulated DE of the extraction means that some light is recirculated within the waveguide to interact with the extraction hologram further.

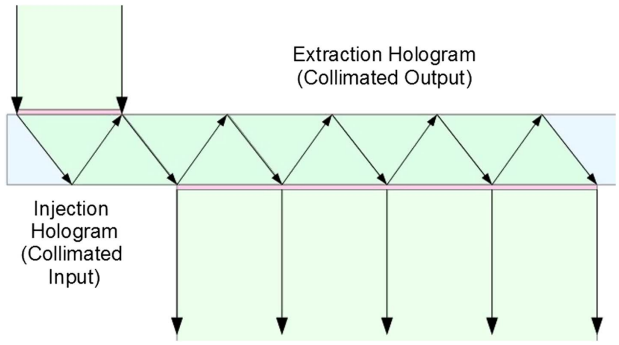

Fig. 3. Schematic of the waveguide configuration. An injection hologram redirects light from the source at TIR along the length of the waveguide. The extraction hologram redirects the internally propagating light toward the observer. Because there is still light propagating within the waveguide after the initial extraction by the extraction hologram, further extractions are possible, which extends the eyebox of the system.

A. Injection Hologram

The injection hologram is designed to receive the light from a source point located at a finite distance from the waveguide surface. The hologram collimates the beam and redirects the light within the waveguide at an angle chosen such that, after one reflection, the left edge of the beam coincides with the right edge of the beam at the injection surface, as presented in Fig. 4. If this condition is not met, the beam will either overlap with itself while propagating within the waveguide or leave dark spaces between the different extractions.

One significant difference between the systems shown in Figs. 3 and 4 is the location of the source point for the injection. In Fig. 3, the incident beam is collimated, which

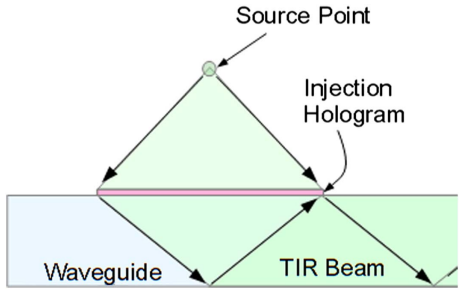

Fig. 4. Light from a source point is collimated and redirected within the waveguide at an angle beyond the critical angle, such that successive reflections are directly adjacent to each other.

corresponds to a source point located in the far field. Figure 4, by contrast, shows a source point located a finite distance from the injection hologram. By using the finite source-point injection system, we are able to locate the projection source for the system at a finite plane. This corresponds to an infinite longitudinal image magnification. Conversely, the projection system for the collimated system needs to be set up to locate the source in the far field. This requires additional lenses in the projection setup, which increases the footprint of the system.

One other advantage of using a short image distance over a collimated injection is an increased field of view (FOV). We were able to demonstrate a FOV of 2° × 2° with a collimated system. In contrast, the system in Fig. 4 has a FOV of 12° × 8°.

B. Extraction Hologram

After propagating through the waveguide, the light is diffracted out of the TIR condition and directed toward the viewer by the extraction hologram, as presented in Fig. 5.

To achieve pupil expansion and ensure uniform intensity along the length of the combiner, the extraction hologram needs to have a modulated DE along its length and must be larger than the size of the injection hologram. This modulated DE means that some of the light is recirculated within the waveguide.

Because the intensity of the light is reduced after each extraction, the variable DE is necessary to maintain uniform intensity across the entire FOV. Each successive portion of the extraction must be more efficient, as less light remains inside the waveguide to be extracted. Thus, the farthest segment of the extraction from the injection hologram must have the maximum DE, as any light remaining in the waveguide after that point is not used. Similarly, the section of the hologram preceding the last extraction must demonstrate 50% DE, such that, of the light in the waveguide at that portion of the extraction, 50% is extracted and redirected to the viewer, while the remaining 50% propagates to the final portion of the extraction and is fully extracted. Equation (1) describes the dependence between the required DE (η_i) for uniform intensity across the extraction, the specific segment number (N_i), and the total number of extraction sections (N_{tot}):

$$\eta_i(N_i, N_{\text{tot}}) = \frac{N_i}{N_{\text{tot}}}. \tag{1}$$

The limitations on the factor of pupil expansion in this system are determined by the desired viewing intensity and the intensity of the source object. Hypothetically, this method could be used to infinitely expand the exit pupil, but the observed intensity would decrease for each additional extraction segment added. Thus, a system with 10× pupil expansion will have, at most, 10% of the incident light visible from each extraction. Figure 6 shows how, for an ideal system with five extractions, the intensity of the light contained within the waveguide decreases, while the required DE increases according to Eq. (1) to maintain uniform intensity along the entire extraction.

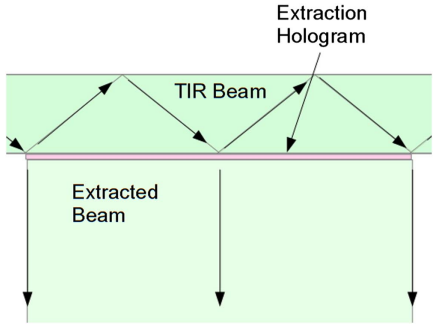

Fig. 5. Collimated light propagating within the waveguide is extracted at the surface normal, presenting a far-field image to the viewer.

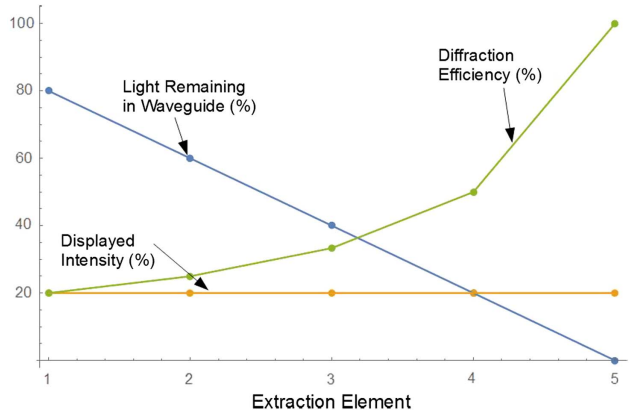

Fig. 6. Ideal DE of the extraction hologram, light intensity inside the waveguide, and display intensity according to location on the combiner. The modulation of the DE compensates for decreasing intensity and maintains uniform image intensity along the entire extraction.

In our system, we demonstrated a 1.7× pupil expansion by having two segments of our extraction. The first segment was 0.7× the size of the injection hologram, and the second was 1× the injection hologram.

3. COMPUTER MODELING

We modeled this optical system in the ray-tracing software Zemax OpticStudio. The model allows for alteration and optimization of the system parameters while analyzing the expected output. The model has an injection hologram written from the interference between the light from a point source and a collimated beam propagating within the waveguide at TIR. Following the injection, the light beams propagate within the waveguide until they are extracted by the second hologram. Figure 7 shows the system with an initial source located at the point used to record the injection hologram. The injection hologram is 90 mm × 90 mm, while the extraction is 150 mm × 90 mm. The injection hologram was recorded from a 350 nm wavelength with the reference source point located 1200 mm behind the injection and a collimated object beam coming into the hologram surface at 67° from the surface normal. The 350 nm wavelength was used because the 532 nm light was propagating through BK7 glass, where the refractive index of the glass compressed the light and reduced the wavelength to 350 nm. The extraction hologram was recorded with its reference beam coming from 67° and diffracting the light normal to the hologram surface. The source point used in

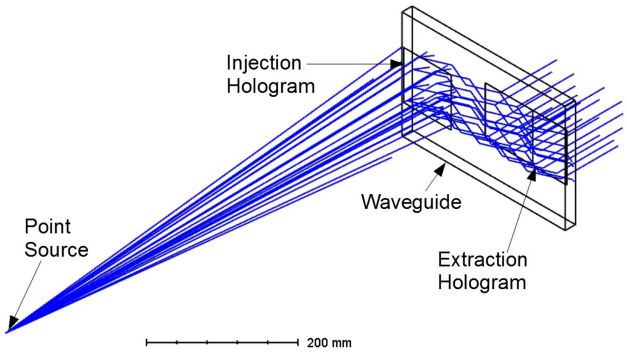

Fig. 7. Isometric view of the Zemax model for our system. The light comes from the same location as the source point used to record the hologram. In that particular case, all diffracted beams exit perpendicular to the waveguide surface.

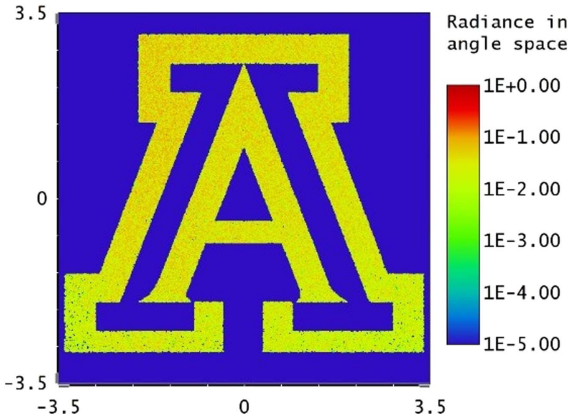

Fig. 9. Angular radiance upon a 3 mm detector square, located 25 cm behind the extraction hologram. The entire injected image is clearly visible through the system.

Fig. 7 has 532 nm wavelength and is located 800 mm from the injection hologram.

To display a full image, the light from an extended source is propagated through the system. Figure 8 shows how the hologram interacts with the light coming from different source points. The injection hologram redirects the light from each source point in a different direction. If the point source is located within some spatial extent, the TIR condition is achieved, and the light from these points is propagated within the waveguide. This is the case for the green and blue colored sources in Fig. 8. Outside this spatial extent, the light is not coupled within the waveguide, and that part of the image will not be visible, as is shown with the red source in the figure.

Figure 9 shows how the light from an extended source propagates through the optical system and is out-coupled toward the viewer's eyes. This ray tracing shows the actual angular radiance on a human pupil-sized detector located 25 cm behind the extraction hologram. The initial image occupies a 110 mm square on the source plane.

In the simulation presented in Fig. 9, the beam is extracted twice from the waveguide by the extraction hologram. This demonstrates that the image is neither multiplied or enlarged by the number of extractions, which is a common misinterpretation of the system mode of operation. Instead, it is the eyebox that is increased. The calculated FOV of the simulated systems is 12° × 8°, and the eyebox is 90 mm × 150 mm with a depth over 1 m.

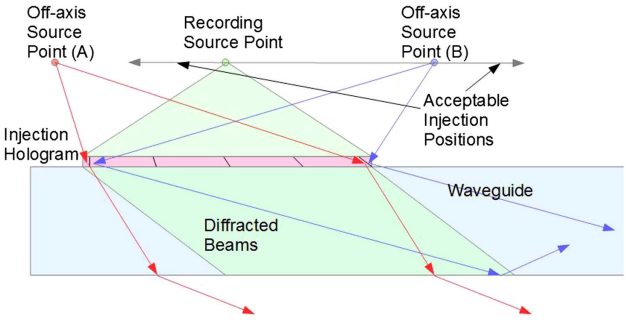

Fig. 8. Schematic of how the injection hologram sends light in different directions depending on the source location. The green arc represents the light from the point source used to record the hologram. The blue arrows demonstrate a source point that is coupled within the waveguide. The red arrows show that some injection locations do not reach the critical angle to couple into the waveguide.

4. PHYSICAL DEMONSTRATOR

After optimizing the parameters for the system using the ray-tracing software, we built a physical demonstrator following the same design. The waveguide is made of Diamant Glass from Saint Gobain, with dimensions of 216 mm × 280 mm× 12 mm. This particular glass type was chosen for its low absorption around the 532 nm wavelength, which can be seen by the low green glare on the edges of the waveguide. We recorded the injection and extraction holograms using Bayfol HX104 photopolymer, a UV curing photopolymer that is easy to apply and has maximum sensitivity around 532 nm recording wavelength.

A. Diffraction Efficiency

As discussed in Section 2, specifically Section 2.B, the DE of the holograms used for the injection and extraction recordings needs to be controlled to maintain uniform intensity over the entirety of the extraction. To that end, we used the dosage of 5 mJ/cm^2 suggested by the manufacturer to record the holograms. This reliably gave a diffraction efficiency of ≈85%. To decrease the diffraction efficiency of the hologram, we used a method of pre-exposure, where the photopolymer is exposed to a single beam of light before the hologram is recorded. This starts the polymerization of the photopolymer before the interference between two beams is recorded and leads to a lower DE of the hologram. Figure 10 shows how the DE of the holograms responded to the pre-exposure energy used. Relative DE refers to the DE compared to a sample recorded without pre-exposure. We measured the relative pre-exposure DE of the photopolymer. The best fit line is given by $\frac{2.6}{E} - 0.26$, where E is the pre-exposure energy, which we used to determine the necessary pre-exposure energy for the system. Thus, we chose to use a 4 mJ pre-exposure in our extraction setup.

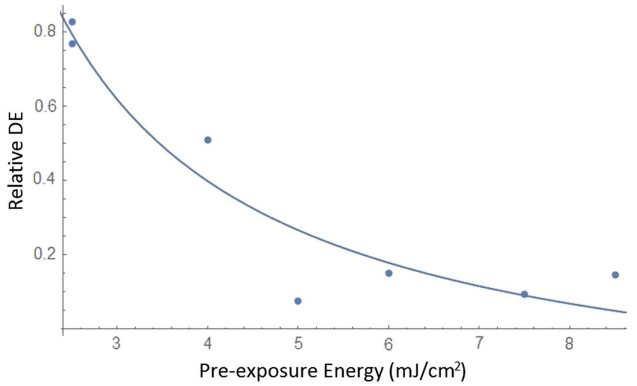

Fig. 10. DE of the photopolymer with different pre-exposure energies.

B. Recording

The recording geometry of the injection hologram follows the incidence angles prescribed by the analysis presented in Section 2.A. The light from the point source is simultaneously collimated and redirected at TIR within the waveguide by the hologram. The hologram is recorded from the interference of two mutually coherent beams from a doubled YAG laser at 532 nm. The reference beam is coming from a diverging point source at normal incidence to the waveguide. The distance of the point source from the injection hologram was chosen so that the diverging beam will fill the injection hologram without having light spill unnecessarily beyond the edges. The object beam is collimated and incident on the waveguide to achieve the TIR angle.

Since the TIR condition implies that the external angle should be 90°, a prism coupler is used to achieve the correct internal angle. However, this prism gets in the way of the reference beam, so we used a pair of 45° prisms in the configuration presented in Fig. 11 to ensure the overlap of the reference and object beams.

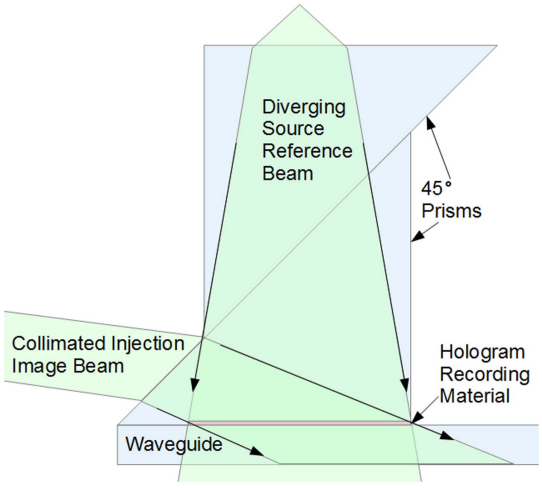

Fig. 11. Injection recording set up to allow for a TIR object beam and a diverging reference beam. In order to make this recording geometry possible, we used a combination of 45° prisms to allow one beam a normal incidence and the other an angled incidence.

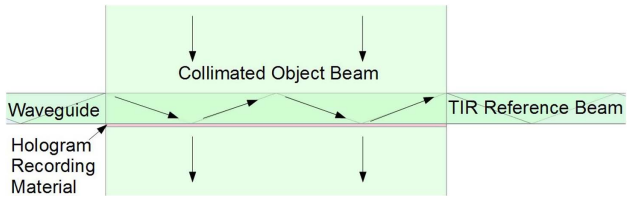

Fig. 12. Extraction hologram is recorded from a normally incident object beam and an internally propagating reference beam. The extraction hologram needs to be recorded with modulated DE to maintain uniform intensity across the entire FOV.

Once we recorded the injection hologram, we illuminated the hologram with a point source and used the resulting collimated, internally propagating beam as the reference beam for the extraction hologram. The object beam was a normally incident plane wave that covers the entire extraction. Figure 12 shows the extraction hologram recording geometry.

As discussed in Section 2.B, the DE of the extraction hologram must be modulated according to the number of sections in the extraction. In the case of our demonstrator, the extraction has two segments, so the first part of the hologram has 50% DE, while the second part has 100% DE. To achieve this different DE, we pre-exposed the first portion of the injection hologram according to the pre-exposure process discussed in Section 4.A. Pre-exposure, in this case, is the process of illuminating the photopolymer with a single beam of light to start the polymerization process in the material without writing a hologram. This lowers the final DE and allows for a single recording for the entire extraction hologram.

C. Testing

In order to test our HUD setup, we constructed the projection system shown in Fig. 13. The light from a projector is focused onto the diffuse plate by a collection lens, while the diffuse plate is located at the source plane for the recording. The injection

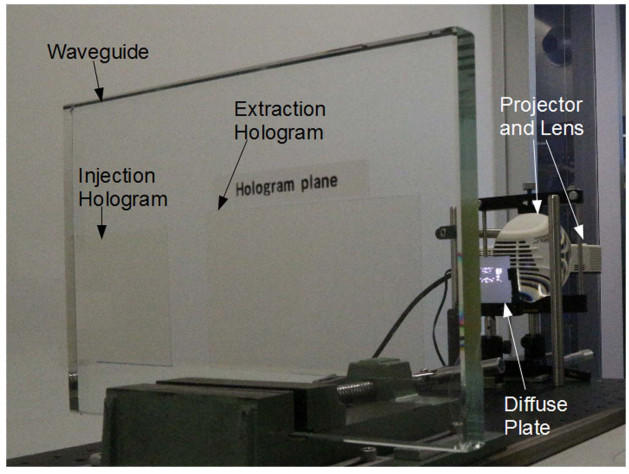

Fig. 13. Picture of the HUD setup, with the waveguide where the injection and extraction holograms are mounted in the foreground. The projection system can be seen in the background.

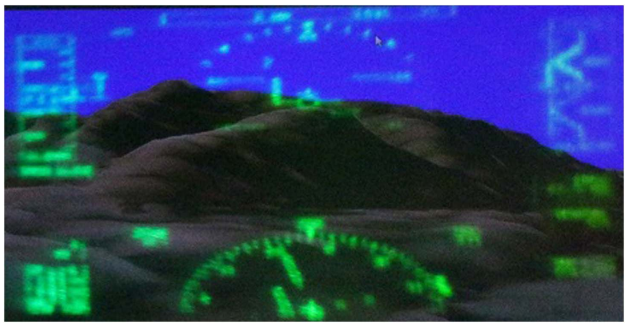

Fig. 14. Picture taken in front of the extraction hologram portion of the HUD. The green flight information is projected through the waveguide system. The hills and sky are a far-field background image displayed on a television set.

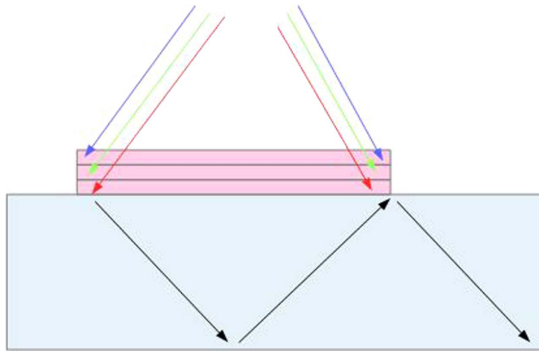

Fig. 15. By recording wavelength selective holograms in different layers, it should be possible to create a full-color waveguide HUD system.

hologram propagates the image through the waveguide where it is visible to the observer through the extraction hologram. It bears noting that we use a collection lens and a diffuse plate only to be able to precisely locate the image plane of the system, which is not possible with the projector by itself. In the case of a system built from the ground up, the projector can be properly designed to take this image plane location directly into account.

Figure 14 is a picture of the image visible through our HUD system. The green flight information is projected through the waveguide. The hills and sky are a background image displayed on a television located several meters away. The entire image is in focus, despite the fact that the background is located much farther away than the hologram plane. This demonstrates that the projected information is also located in the far field, and the viewer does not need to re-accommodate his/her eyes to look at it. There are two sources for the lack of sharpness in the projected image. First is the quality of the holographic backing medium, which is a polymer film that induces some distortion. This can be addressed by using a higher-quality holographic recording medium, such as dichromated gelatin (DCG). The second source of fuzziness is due to the difference in the locations of the background image and the projected symbology. Our HUD system projects the symbology into the far field, but the background image is located only 10 m behind the hologram. We focused on the background image, as opposed to the hologram symbology. This can be solved by increasing the optical power of the projection system and extending the distance between the hologram plane and the background image.

5. POSSIBLE FUTURE WORK: FULL-COLOR HUD SYSTEM

Despite the fact that we used a polychromatic RGB projection system, the image relayed by the waveguide is green and monochromatic. This is because the injection and extraction holograms act as notch filters, diffracting only the green portion of the spectrum, while other wavelengths pass through unaffected. To obtain a full-color system, three holograms would need to be recorded for both the injection and extraction segments. These three holograms would individually diffract the red, green, and blue colors, as shown in Fig. 15. These holograms do not need to be recorded separately, and can be multiplexed inside the same material, provided that the material is sensitive to these wavelengths. For this display effort, we will be able to take advantage of full-color holographic display systems [22,23] for injecting the source image into our waveguide system.

One such material that would allow for this multiplexed hologram recording is Bayfol HX200, which can be recorded with light from 440 nm to 671 nm, according to the data sheet. To realize a full-color system, we could either apply, record, and develop a hologram for each color individually or multiplex the hologram into a single layer of the photopolymer.

6. CONCLUSION

In this paper, we demonstrated that it is possible to achieve both pupil expansion and longitudinal image magnification simultaneously, using holograms and waveguide optics. The magnification is provided by the optical power implemented in the injection hologram, whereas the pupil expansion is due to the multiple extractions of the light out of the waveguide by the extraction hologram. A ray-tracing model was developed in Zemax to optimize the geometry of the holograms with respect to the size and location of the image source. The proof-of-concept system we presented has an infinite longitudinal magnification and a pupil expansion of 1.7×. This FOV can be expanded by increasing the size of the injection and extraction hologram elements. Also, increasing the divergence of the source point beam used for the injection recording can minimize the form factor of the projection system. Appropriate design of the projection system would eliminate the need for a separate intermediate image plane can also reduce the size of the projection system.

Funding. Honeywell Labs (6400282571, 6400327460).

Acknowledgment. The authors would like to thank Brian Redman, Dave Sommitz, Benjamin Cromey, Brittany Arviso, Dr Yuzuru Takashima, and Dr Lloyd LaComb for their valuable input throughout the research process.

REFERENCES

1. Y.-C. Liu and M.-H. Wen, "Comparison of head-up display (HUD) vs. head-down display (HDD): driving performance of commercial vehicle operators in Taiwan," Int. J. Hum. Comput. Stud. **61**, 679–697 (2004).
2. M. AblaBmeier, T. Poitschke, F. W. K. Bengler, and G. Rigoll, "Eye gaze studies comparing head-up and head-down displays in vehicles," in *IEEE International Conference on Multimedia and Expo* (2007), pp. 2250–2252.
3. C. Wickens and P. Ververs, "Allocation of attention with head-up displays," Tech. Rep. DOT/FAA/AM-98/28 (Aviation Research Laboratory, Institute of Aviation, 1998).
4. S. Fadden, C. D. Wickens, and P. Ververs, "Costs and benefits of head up displays: an attention perspective and a meta analysis," in *SAE Technical Paper* (SAE International, 2000).
5. W. J. Horrey, C. D. Wickens, and A. L. Alexander, "The effects of head-up display clutter and in-vehicle display separation on concurrent driving performance," Proc. Hum. Factors Ergon. Soc. Annu. Meet. **47**, 1880–1884 (2003).
6. P. Coni, S. Hourlier, A. Gueguen, X. Servantie, and L. Laluque, "50-3: a full windshield head-up display using simulated collimation," SID Symp. Dig. Tech. Pap. **47**, 684–687 (2016).
7. P. Coni, S. Hourlier, X. Servantie, L. Laluque, and A. Gueguen, "A 3D head up display with simulated collimation," in *SAE Technical Paper* (SAE International, 2016).
8. J. Han, J. Liu, X. Yao, and Y. Wang, "Portable waveguide display system with a large field of view by integrating freeform elements and volume holograms," Opt. Express **23**, 3534–3549 (2015).
9. J. Upatnieks, "Compact head-up display," U.S. patent 4,711,512 (8 December 1987).
10. R. B. Wood and M. J. Hayford, "Holographic and classical head up display technology for commercial and fighter aircraft," Proc. SPIE **0883**, 36–52 (1988).
11. H. Kato, H. Ito, J. Shima, M. Imaizumi, and H. Shibata, "Development of hologram head-up display," in *SAE Technical Paper* (SAE International, 1992).
12. M. H. Kalmanash, "Digital HUDs for tactical aircraft," Proc. SPIE **6225**, 6225OL (2006).
13. H. Peng, D. Cheng, J. Han, C. Xu, W. Song, L. Ha, J. Yang, Q. Hu, and Y. Wang, "Design and fabrication of a holographic head-up display with asymmetric field of view," Appl. Opt. **53**, H177–H185 (2014).
14. C. H. Vallance, "The approach to optical system designs for aircraft head up displays," Proc. SPIE **0399**, 15–25 (1983).
15. C. T. Bartlett, M. L. Busbridge, and O. T. Horton, "Considerations of a head-up display field of view," Proc. SPIE **4712**, 468–479 (2002).
16. P. L. Wisely, "Head up and head mounted display performance improvements through advanced techniques in the manipulation of light," Proc. SPIE **7327**, 732706 (2009).
17. J. A. Cox, T. A. Fritz, and T. R. Werner, "Application and demonstration of diffractive optics for head-mounted displays," Proc. SPIE **2218**, 32–40 (1994).
18. A. A. Cameron, "Optical waveguide technology and its application in head-mounted displays," Proc. SPIE **8383**, 83830E (2012).
19. S. D. Harbour, "Three-dimensional system integration for HUD placement on a new tactical airlift platform: design eye point vs. HUD eye box with accommodation and perceptual implications," Proc. SPIE **8383**, 83830V (2012).
20. M. Homan, "The use of optical waveguides in head up display (HUD) applications," Proc. SPIE **8736**, 87360E (2013).
21. I. K. Wilmington and M. S. Valera, "Paper no 18.2: waveguide-based display technology," SID Symp. Dig. Tech. Pap. **44**, 278–280 (2013).
22. N. Mohammad, M. Meem, X. Wan, and R. Menon, "Full-color, large area, transmissive holograms enabled by multi-level diffractive optics," Sci. Rep. **7**, 5789 (2017).
23. J. Roh, K. Kim, E. Moon, S. Kim, B. Yang, J. Hahn, and H. Kim, "Full-color holographic projection display system featuring an achromatic Fourier filter," Opt. Express **25**, 14774–14782 (2017).